RNASeq analysis identifies non-canonical role of STAT2 and IRF9 in the regulation of a STAT1-independent antiviral and immunoregulatory transcriptional program induced by IFNβ and TNFα

Mélissa K. Mariani[1], Pouria Dasmeh[2,3], Audray Fortin[1], Mario Kalamujic[1], Elise Caron[1], Alexander N. Harrison[1,4] Sandra Cervantes-Ortiz[1,5], Espérance Mukawera[1], Adrian W.R. Serohijos[2,3] and Nathalie Grandvaux[1,2]*

[1] CRCHUM - Centre Hospitalier de l'Université de Montréal, Québec, Canada
[2] Department of Biochemistry and Molecular Medicine, Faculty of Medicine, Université de Montréal, Qc, Canada.
[3] Centre Robert Cedergren en Bioinformatique et Génomique, Université de Montréal, Qc, Canada
[4] Department of Microbiology and Immunology, McGill University, Qc, Canada
[5] Department of Microbiology, Infectiology and Immunology, Faculty of Medicine, Université de Montréal, Qc, Canada

*** Correspondence:**
Corresponding Author
nathalie.grandvaux@umontreal.ca

Keywords: Interferon β, TNFα, STAT1, STAT2, IRF9, antiviral,

Running title: STAT1-independent transcriptional response to IFNβ+TNFα

ABSTRACT

IFNβ plays a critical role in the host defense against pathogens through the induction of hundreds of antiviral and immunoregulatory genes. Response to IFNβ is context-dependent and is prone to crosstalk with other cytokines. Costimulation with IFNβ and TNFα drives a specific delayed transcriptional program composed of genes that are either not responsive to IFNβ or TNFα separately or are only responsive to either one of the cytokine. The signaling mechanisms engaged downstream of the costimulation with IFNβ and TNFα remained elusive. In the present study, we took advantage of STAT1-deficient cells coupled to RNASeq analysis to characterize the genome wide transcriptional profile induced in response to IFNβ and TNFα. We found that costimulation with IFNβ and TNFα induces a broad antiviral and immunoregulatory transcriptional program independently of STAT1. Additional sequencing performed following silencing of STAT2 or IRF9 allowed us to unveil specific independent roles of STAT2 and IRF9 in the regulation of distinct sets of IFNβ and TNFα-induced genes. Consistent with the growing literature, IFNβ and TNFα synergistic action is in part mediated by the concerted action of STAT2 and IRF9, most likely present in a non-canonical complex. Finally, our study reveals previously unrecognized independent roles of STAT2 and IRF9 in the regulation of distinct sets of IFNβ and TNFα-induced genes. Altogether these observations highlight novel STAT1-independent pathways involved in the establishment of a delayed antiviral and immunoregulatory transcriptional program in conditions where elevated levels of both IFNβ and TNFα are present.

INTRODUCTION

Interferon (IFN) β plays a critical role in the first line of defense against pathogens, particularly viruses, through its ability to induce a broad antiviral transcriptional response in virtually all cell types (*1*). IFNβ also possesses key immunoregulatory functions that determine the outcome of the adaptive immune response against pathogens (*1, 2*). IFNβ acts through binding to the IFNAR receptor (IFNAR1 and IFNAR2) leading to Janus kinases (JAK), JAK1 and Tyk2, mediated phosphorylation of signal transducer and activator of transcription (STAT) 1 and STAT2, and to a lesser extent other STAT members in a cell-specific manner (*3, 4*). Phosphorylated STAT1 and STAT2 together with IFN Regulatory Factor (IRF) 9 form the IFN-stimulated gene factor 3 (ISGF3) complex that binds to the consensus IFN-stimulated response element (ISRE) sequences in the promoter of hundreds of IFN stimulated genes (ISGs) (*5*). Formation of the ISGF3 complex is considered a hallmark of the engagement of the type I IFN response, and consequently the requirement of STAT1 in a specific setting has become a marker of the engagement of type I IFN signaling (*3, 6*). However, in recent years this paradigm has started to be challenged with accumulating evidence demonstrating the existence of non-canonical JAK-STAT signaling mediating type I IFN responses (*4, 7*).

Over the years, *in vitro* and *in vivo* studies aimed at characterizing the mechanisms and the functional outcomes of IFNβ signaling were mostly performed in relation to single cytokine stimulation. However, this unlikely reflects physiological settings, as a plethora of cytokines is secreted in a specific situation. As a consequence, a cell rather simultaneously responds to a cocktail of cytokines to foster the appropriate transcriptional program. Response to IFNβ is no exception and is very context-dependent, particularly regarding the potential cross-talk with other cytokines. IFNβ and TNFα exhibit context-dependent cross-regulation, but elevated levels of both cytokines are found during the host response to pathogens, including virus and bacteria, and also in autoinflammatory and autoimmune diseases (*8*). While the cross-regulation of IFNβ and TNFα is well studied, the functional cross-talk between these two cytokines remains poorly known and is limited to the description of a synergistic interaction (*9-12*). Indeed, costimulation with IFNβ and TNFα was found to drive a specific delayed transcriptional program composed of genes that are either not responsive to IFNβ or TNFα separately or are only responsive to either one of the cytokine (*10, 11*).

The signaling mechanisms engaged downstream of the costimulation with IFNβ and TNFα remained elusive, but it is implicitly assumed that the fate of the gene expression response requires that both IFNβ and TNFαinduced signaling pathways exhibit significant cross-talk. Analysis of the enrichment of specific transcription factors binding sites in the promoters of a panel of genes synergistically induced by IFNβ and TNFα failed to give a clue about the specificity of the transcriptional regulation of these genes (*10*). Recently, analysis of the induction of *DUOX2 and DUOXA2* genes, which belong to the category of delayed genes that are remarkably induced to high levels in response to the combination of IFNβ and TNFα, led to the hypothesis that STAT2 and IRF9 activities might segregate in an alternative STAT1-independent pathway that could be involved in gene induction downstream of IFNβ and TNFα (*12*). Further validation was awaited to confirm the existence of this STAT1-independent response and the extent to which it is involved in the regulation of a specific delayed transcriptional program induced by the combination of IFNβ and TNFα.

In the present study, we aimed to characterize the transcriptional profile of the delayed response to IFNβ and TNFα in the absence of STAT1. Taking advantage of STAT1-deficient cells,

we found that costimulation with IFNβ and TNFα induces a broad antiviral and immunoregulatory transcriptional program. Furthermore, we evaluated the contribution of STAT2- and IRF9-dependent pathway(s) in the regulation of this delayed transcriptional response. Importantly, numerous genes were found to be independent of STAT2 and IRF9. We report that STAT2 and IRF9 are differentially involved in the regulation of distinct subsets of genes induced by IFNβ+TNFα. Our findings also highlight the role of distinct non-canonical STAT2 and/or IRF9 pathways; while IFNβ and TNFα synergistic action is in part mediated by the concerted action of STAT2 and IRF9, our study also reveals specific independent roles of STAT2 and IRF9 in the regulation of distinct sets of genes.

MATERIAL AND METHODS

Cell culture and stimulation

A549 cells (American Type Culture Collection, ATCC) were grown in F-12 nutrient mixture (Ham) medium supplemented with 10% heat-inactivated fetal bovine serum (HI-FBS) and 1% L-glutamine. 2FTGH fibrosarcoma cell line derived U3A (STAT1-deficient) and U3AR (STAT1 rescued U3A), a generous gift from Dr. G. Stark, Cleveland, USA (*13*), were grown in DMEM medium supplemented with 10% HI-FBS, 1% L-glutamine. All cell lines were cultured without antibiotics. All media and supplements were from Gibco. Mycoplasma contamination was excluded by regular analysis using the MycoAlert Mycoplasma Detection Kit (Lonza). Cells were stimulated with IFNβ (1000 U/mL, PBL Assay Science), TNFα (10 ng/mL, R&D Systems) or IFNβ (1000 U/mL) +TNFα (10 ng/mL) for the indicated times.

siRNA Transfection

The sequences of non-targeting control (Ctrl) and STAT2- and IRF9-directed RNAi oligonucleotides (Dharmacon, USA) have previously been described in (*12*). U3A cells at 30% confluency were transfected using the Oligofectamine transfection reagent (Life technologies). RNAi transfection was pursued for 48 h before stimulation.

Immunoblot analysis

Cells were lysed on ice using Nonidet P-40 lysis buffer as fully detailed in (*14*). Whole-cell extracts (WCE) were quantified using the Bradford protein assay (Bio-Rad), resolved by SDS-PAGE and transferred to nitrocellulose membrane before analysis by immunoblot. Membranes were incubated with the following primary antibodies, anti-actin Cat #MAB1501 from Millipore, anti-IRF9 Cat #610285 from BD Transduction Laboratories, and anti-STAT1-P-Tyr701 Cat #9171, anti-STAT2-P-Tyr690 Cat #4441, anti-STAT1 Cat #9172, anti-STAT2 Cat #4594, all from Cell Signaling, before further incubation with horseradish peroxidase (HRP)-conjugated secondary antibodies (KPL or Jackson Immunoresearch Laboratories). Antibodies were diluted in PBS containing 0.5% Tween and either 5% nonfat dry milk or BSA. Immunoreactive bands were visualized by enhanced chemiluminescence (Western Lightning Chemiluminescence Reagent Plus, Perkin-Elmer Life Sciences) using a LAS4000mini CCD camera apparatus (GE healthcare).

RNA isolation and qRT-PCR analyses

Total RNA was prepared using the RNAqueous-96 Isolation Kit (Ambion) following the manufacturer's instructions. Total RNA (1µg) was subjected to reverse transcription using the QuantiTect Reverse Transcription Kit (Qiagen). Quantitative PCR were performed using either Fast start SYBR Green Kit (Roche) for *Mx1*, *IDO*, *APOBEC3G*, *CXCL10*, *NOD2*, *PKR*, *IRF1*, and *IFIT1* and *IL8* or TaqMan Gene Expression Assays (Applied Biosystems) for *DUOX2*, *IFI27*, *SERPINB2*, *IL33*, *CCL20*, *ISG20*, *OAS3*, *GRB14*, *CLEC5A*, *DGX58*, *ICAM1*, *IL1B*, *JUNB*, *MMP9*, *SERPINA1*

and HERC6. Sequences of oligonucleotides and probes used in PCR reactions are described in **Supplemental Table S4**. Data collection was performed on a Rotor-Gene 3000 Real Time Thermal Cycler (Corbett Research). Gene inductions were normalized over S9 levels, measured using Fast start SYBR Green Kit or TaqMan probe as necessary. Fold induction of genes was determined using the ΔΔCt method (*15*). All qRT-PCR data are presented as the mean ± SEM.

RNA-sequencing (RNASeq)

Total RNA prepared as described above was quantified using a NanoDrop Spectrophotometer ND-1000 (NanoDrop Technologies, Inc.) and its integrity was assessed using a 2100 Bioanalyzer (Agilent Technologies). Libraries were generated from 250 ng of total RNA using the NEBNext poly(A) magnetic isolation module and the KAPA stranded RNA-Seq library preparation kit (Kapa Biosystems), as per the manufacturer's recommendations. TruSeq adapters and PCR primers were purchased from IDT. Libraries were quantified using the Quant-iT™ PicoGreen® dsDNA Assay Kit (Life Technologies) and the Kapa Illumina GA with Revised Primers-SYBR Fast Universal kit (Kapa Biosystems). Average size fragment was determined using a LabChip GX (PerkinElmer) instrument. Massively parallel sequencing was carried out on an Illumina HiSeq 2500 sequencer. Read counts were obtained using HTSeq. Reads were trimmed from the 3' end to have a Phred score of at least 30. Illumina sequencing adapters were removed from the reads and all reads were required to have a length of at least 32bp. Trimming and clipping was performed using Trimmomatic (*16*). The filtered reads were aligned to the Homo-sapiens assembly GRCh37 reference genome. Each readset was aligned using STAR (*17*) and merged using Picard (http://broadinstitute.github.io/picard/). For all samples, the sequencing resulted in more than 29 million clean reads (ranging from 29 to 44 million reads) after removing low quality reads and adaptors. The reads were mapped to the total of 63679 gene biotypes including 22810 protein-coding genes. The non-specific filter for 1 count-per million reads (CPM) in at least three samples was applied to the reads and 14,254 genes passed this criterion. The entire set of RNAseq data has been submitted to the Gene Expression Omnibus (GEO) database (http://www.ncbi.nlm.nih.gov/geo) under accession number GSE111195.

Bioinformatics analysis

Differential transcripts analysis. A reference-based transcript assembly was performed, which allows the detection of known and novel transcripts isoforms, using Cufflinks (*18*), merged using Cuffmerge (cufflinks/AllSamples/merged.gtf) and used as a reference to estimate transcript abundance and perform differential analysis using Cuffdiff and Cuffnorm tool to generate a normalized data set that includes all the samples. FPKM values calculated by Cufflinks were used as input. The transcript quantification engine of Cufflinks, Cuffdiff, was used to calculate transcript expression levels in more than one condition and test them for significant differences. To identify a transcript as being differentially expressed, Cuffdiff tests the observed log-fold-change in its expression against the null hypothesis of no change (i.e. the true log-fold-change is zero). Because of measurement errors, technical variability, and cross-replicate biological variability might result in an observed log-fold-change that is non-zero, Cuffdiff assesses significance using a model of variability in the log-fold-change under the null hypothesis. This model is described in details in (*19*). The differential gene expression analysis was performed using DESeq (*20*) and edgeR (*21*) within the R Bioconductor packages. Genes were considered differentially expressed between two group if they met the following requirement: fold change (FC) > ±1.5, $p<0.05$, FDR <0.05.

Enrichment of gene ontology (GO). GO enrichment analysis amongst differentially expressed genes (DEGs) was performed using Goseq (*22*) against the background of full human genome (hg19). GO-terms with adjusted p value < 0.05 were considered significantly enriched.

Clustering of DEGs. We categorized the DEGs according to their response upon silencing of siSTAT2 and siIRF9; categories are listed as A to I (Figure 2E). Then to determine relationship between these categories, we calculated the distance of centers of different categories. For each gene,

we transformed siSTAT2 and siIRF9 fold changes (FC) to deviation from the mean FC of the category the respective gene belongs: $FC_{new} = FC_{old} - \varepsilon (FC_{category})$. The parameter ε was estimated to give the perfect match between predefined categories (A to I) and clustering based on Euclidean distance. Results were plotted as a heatmap.

Modular transcription analysis. The *tmod* package in R (*23*) was used for modular transcription analysis. In brief, each transcriptional module is a set of genes, which shows coherent expression across many biological samples (*24*, *25*). Modular transcription analysis then calculates significant enrichment of a set of foreground genes, here DEGs, in pre-defined transcriptional module compared to a reference set. For transcriptional modules, we used a combined list of 606 distinct functional modules encompassing 12712 genes, defined by Chaussabel et al. (*26*) and Li et al. (*27*), as the reference set in tmod package (**Supplemental table S5**). The hypergeometric test devised in *tmodHGtest* was used to calculate enrichments and p-values employing Benjamini-Hochberg correction (*28*) for multiple sampling. All the statistical analyses and graphical presentations were in performed in R (*29*).

Luciferase gene reporter assay

U3A or U3AR cells at a confluency of 90% were cotransfected with 100 ng of one of the following CXCL10 promoter containing firefly luciferase reporter plasmids (generously donated by Dr. David Proud, Calgary, (*30*)), CXCL10prom-972pb-pGL4 (full length -875/+97 promoter), CXCL10prom-376pb-pGL4 (truncated -279/+97 promoter), CXCL10prom972pb-ΔISRE(3)-pGL4 (full length promoter with ISRE(3) site mutated), CXCL10prom972pb-ΔκB(1)-pGL4 (full length promoter with NFκB(1) site mutated), CXCL10prom972pb-ΔκB(2)-pGL4 (full length promoter with NFκB(2) site mutated), CXCL10prom972pb-ΔAP-1-pGL4 (full length promoter with AP-1 site mutated) together with 50ng of pRL-null renilla-luciferase expressing plasmid (internal control). Transfection was performed using Lipofectamine 2000 (Life technologies) using a 1:2 DNA to lipofectamine ratio. At 8 h post-transfection, cells were stimulated for 16 h with either IFNβ (1000 U/mL) or IFNβ+TNFα (1000 U/mL;10 ng/mL) as indicated. Firefly and renilla luciferase activities were quantified using the Dual-luciferase reporter assay system (Promega). Luciferase activities were calculated as the luciferase/renilla ratio and were expressed as fold over the non-stimulated condition.

Statistical analyses

Statistical analyses of qRT-PCR and luciferase assay results were performed using the Prism 7 software (GraphPad) using the tests indicated in the figure legends. Statistical significance was evaluated using the following P values: $P < 0.05$ (*), $P < 0.01$ (**), $P < 0.001$ (***) or $P < 0.0001$ (****). Differences with a P-value < 0.05 were considered significant. Statistical analysis of the RNASeq data is described in the Bioinformatics analysis section above.

RESULTS

Distinct induction profiles of antiviral and immunoregulatory genes in response to IFNβ, TNFα and IFNβ+TNFα.

First, we sought to determine the induction profile of a selected panel of immunoregulatory and antiviral genes in response to IFNβ+TNFα in comparison to TNFα or IFNβ alone. A549 cells were stimulated either with TNFα, IFNβ or IFNβ+TNFα for various times between 3-24h and the relative mRNA expression levels were quantified by qRT-PCR. Analysis of the expression of the selected genes revealed distinct profiles of response to TNFα, IFNβ or IFNβ+TNFα (**Figure 1**).

IDO, DUOX2, CXCL10, APOBEC3G, ISG20 and IL33 exhibited synergistic induction in response to IFNβ+TNFα compared to TNFα or IFNβ alone. Expression in response to IFNβ+TNFα increased over time, with maximum expression levels observed between 16 and 24h. While *NOD2* and IRF1 induction following stimulation with IFNβ+TNFα was also significantly higher than upon IFNβ or TNFα single cytokine stimulation, they exhibited a steady-state induction profile starting as early as 3h. *MX1* and *PKR*, two typical ISGs, were found induced by IFNβ+TNFα similarly to IFNβ alone and were not responsive to TNFα. *CCL20* responded to IFNβ+TNFα with a kinetic and amplitude similar to TNFα, but was not responsive to IFNβ alone. *IL8* expression was not induced by IFNβ, but was increased by TNFα starting at 3h and remained steady until 24h. In contrast to other genes, *IL8* induction in response to IFNβ+TNFα was significantly decreased compared to TNFα alone. Overall, these results confirm that induction of a subset of antiviral and immunoregulatory genes is greatly increased in response to IFNβ+TNFα compared to either IFNβ or TNFα alone.

Workflow for genome-wide characterization of the delayed transcriptional program induced by IFNβ+TNFα in the absence of STAT1.

In a previous report, we provided evidence of a STAT1-independent, but STAT2- and IRF9-dependent, pathway engaged downstream of IFNβ+TNFα (*12*). Here, taking advantage of the STAT1-deficient human U3A cell line (*13*), we aimed to fully characterize the STAT1-independent transcriptional program induced by IFNβ+TNFα. Two hallmarks of STAT2 and IRF9 activation, *i.e.* STAT2 Tyr690 phosphorylation and induction of IRF9, were observed in U3A cells following stimulation with IFNβ+TNFα. Although STAT2 and IRF9 activation was reduced compared to U3AR cells expressing STAT1, this observation supports the capacity of STAT2 and IRF9 to be activated in STAT1-deficient U3A cells stimulated with IFNβ+TNFα (**Figure 2A**).

To investigate the transcriptional program triggered independently of STAT1, the U3A cells were efficiently transfected with Control (Ctrl)-, STAT2- or IRF9-RNAi and further left untreated or stimulated with IFNβ+TNFα for 16h (**Figure 2B**). Efficient silencing was confirmed by immunoblot (**Figure 2C**). To perform genome-wide transcriptional analysis, total RNA was isolated and analyzed by RNA sequencing (n=3 for each group detailed in **Figure 2B**) on an Illumina HiSeq2500 platform. To validate the RNASeq data, the fold changes (FC) of 13 genes between the different experimental groups, siCTRL non-stimulated (NS) *vs* siCTRL IFNβ+TNFα, siCTRL IFNβ+TNFα *vs* siSTAT2 IFNβ+TNFα and siCTRL IFNβ+TNFα *vs* siIRF9 IFNβ+TNFα was confirmed by qRT-PCR. A positive linear relationship between RNASeq and qRT-PCR FC was observed (**Figure 2D**).

An antiviral and immunoregulatory transcriptional signature is induced by IFNβ+TNFα independently of STAT1.

To identify STAT1-independent differentially expressed genes (DEGs) upon IFNβ+TNFα stimulation, comparison between non-stimulated (NS) and IFNβ+TNFα stimulated control cells was performed (**Figure 2E**). In total, 612 transcripts, including protein-coding transcripts, pseudogenes and long non-coding RNA (lncRNA), were significantly different (Fold change (FC) >1.5, $p<0.05$, FDR <0.05) in IFNβ+TNFα *vs* NS. Among these, 482 DEGs were upregulated and 130 were downregulated (**Figure 3A;** See **Supplemental Table S1** for a complete list of DEGs). To identify the Biological Processes (BP) and Molecular Functions (MF) induced by IFNβ+TNFα independently of STAT1, we first subjected upregulated DEGs through Gene Ontology (GO) enrichment analysis. The top enriched GO BP (p-value < 10^{-10}) and MF, are depicted in **Figure 3B (**See **Supplemental Table S2** for a complete list of enriched GO). The majority of the top enriched BPs were related to cytokine production and function (response to cytokine, cytokine-mediated signaling pathway,

cytokine production, regulation of cytokine production), immunoregulation (Immune response, immune system process, innate immune response, regulation of immune system process) and host defense response (defense response, response to other organism, 2'-5'-oligoadenylate synthetase activity and dsRNA binding). Fourteen MF categories were found enriched in IFNβ+TNFα. The top enriched MFs were related to cytokine and chemokine functions (cytokine activity, cytokine receptor binding, chemokine activity, Interleukin 1-receptor binding). Other enriched MF included peptidase related functions (endopeptidase inhibitor activity, peptidase regulator activity, serine-type endopeptidase activity).

To further gain insight into the functional significance of the IFNβ+TNFα-induced transcriptional response, we conducted a modular transcription analysis of upregulated DEGs against 606 immune-related functional modules. These modules were previously defined from co-clustered gene sets built via an unbiased data-driven approach as detailed in the material and methods section (*26, 27*). IFNβ+TNFα-induced DEGs showed significant enrichment in 37 modules (**Supplemental Table S3**). Six of these modules were associated with virus sensing/Interferon antiviral response, including LI.M75 (antiviral IFN signature), LI.M68 (RIG-I-like receptor signaling), LI.M127 (type I interferon response), LI.M111.0 and LI.M111.1 (IRF2 target network) and LI.M150 (innate antiviral response) (**Figure 3C**). Additionally, 6 modules were associated with immunoregulatory functions, including LI.M29 (proinflammatory cytokines and chemokines), LI.M27.0 and LI.M27.1 (chemokine cluster I and II), LI.M38 (chemokines and receptors), LI.M115 (cytokines receptors cluster) and LI.M37.0 (immune activation - generic cluster) (**Figure 3C**). Module analysis also showed enriched AP-1 transcription factor-related network modules, LI.M20 and LI.M0, and cell cycle and growth arrest LI.M31 module. Collectively, these data demonstrate that the co-stimulation with IFNβ and TNFα induces a broad antiviral and immunoregulatory transcriptional program that is independent of STAT1.

Clustering of STAT1-independent IFNβ+TNFα induced DEGs according to their regulation by STAT2 and IRF9.

Next, we sought to assess how the STAT1-independent IFNβ+TNFα-induced antiviral and immunoregulatory transcriptional response was regulated by STAT2 and IRF9. To do so, we compared transcripts levels in siSTAT2_IFNβ+TNFα *vs* siCTRL_IFNβ+TNFα and siIRF9_IFNβ+TNFα *vs* siCTRL_IFNβ+TNFα conditions (**Figure 2E** and **Supplemental Table S1**). Volcano plots revealed that a fraction of IFNβ+TNFα-induced DEGs were significantly (Fold change (FC) >1.5, $p<0.05$, FDR <0.05) downregulated or upregulated upon silencing of STAT2 (**Figure 4A**) or IRF9 (**Figure 4B**). Nine distinct theoretical categories of DEGs can be defined based on their potential individual behavior across siSTAT2 and siIRF9 groups (Categories A-I, **Figure 2E**): a gene can either be downregulated upon STAT2 and IRF9 silencing, indicative of a positive regulation by STAT2 and IRF9 (Categorie A); conversely, a gene negatively regulated by STAT2 and IRF9 would exhibit upregulation upon STAT2 and IRF9 silencing (Categorie B); Genes that do not exhibit significant differential expression in siSTAT2 and siIRF9 groups would be classified as STAT2 and IRF9 independent (Categorie C); IRF9-independent genes could exhibit positive (Categorie D) or negative (Categorie E) regulation by STAT2; conversely, STAT2-independent genes might be positively (Categorie F) or negatively (Category G) regulated by IRF9; lastly, STAT2 and IRF9 could have opposite effects on a specific gene regulation (Categorie H and I). Based on *a priori* clustering of RNASeq data (**Figure 4C**) and analysis of the expression of 18 genes by qRT-PCR (**Figure 4D**), we found that IFNβ+TNFα-induced DEGs clustered into only 7 of the 9 possible categories. A large majority of upregulated DEGs, i.e. 319 out of the 482 DEGs, were not

significantly affected by either STAT2 or IRF9 silencing, and were therefore classified as STAT2/IRF9 independent (**Figure 4C**). The remaining upregulated DEGs exhibited either inhibition or upregulation following silencing of STAT2 and/or IRF9 (Category B-G). No genes were found in categorie H and only one gene was found in categorie I.

To functionally interpret these clusters, we applied the modular transcription analysis to each of the categories to assess for the specific enrichment of the functional modules found associated with IFNβ+TNFα-upregulated DEGs (**Figure 4E**). First, all modules were found enriched in the cluster of genes induced independently of STAT2 and IRF9 (Category C), pointing to a broad function of this yet to be defined pathway(s) in the regulation of the antiviral and immunoregulatory program elicited by IFNβ+TNFα. Similarly, most modules, except LI.M31 (cell cycle and growth arrest), LI.M38 (chemokines and receptors), LI.M37.0 (immune activation - generic cluster) and LI.M53 (inflammasome receptors and signaling), were enriched in the category of DEGs positively regulated by STAT2 and IRF9 (Category A). Conversely, the cluster negatively regulated by STAT2 and IRF9 (Category B) exclusively contains enriched LI.M38 (chemokines and receptors), LI.M37.0 (immune activation - generic cluster) and LI.M115 (cytokines receptors cluster). The cluster of IRF9-independent genes that are negatively regulated by STAT2 (Category E) only exhibited enrichment in the virus sensing/ IRF2 target network LI.M111.0 module, while the IRF9-independent/ STAT2-positively regulated cluster (Category D) encompasses antiviral and immunoregulatory functions. The STAT2-independent, but IRF9 positively regulated transcripts (Category F) was mainly enriched in modules associated with the IFN antiviral response, including LI.M75 (antiviral IFN signature), LI.M68 (RIG-I-like receptor signaling), LI.M127 (type I interferon response), and LI.M150 (innate antiviral response). Finally, the STAT2-independent, but IRF9 negatively regulated cluster (Category G) was mostly enriched in modules associated with immunoregulatory functions, including LI.M29 (proinflammatory cytokines and chemokines), LI.M27.0 and LI.M27.1 (chemokine cluster I and II), LI.M78 (myeloid cell cytokines), but also with cell cycle and growth arrest (LI.M31) and inflammasome receptors and signaling (LI.M53). Altogether these observations reveal that STAT2 and IRF9 are involved in the regulation of only a subset of the genes induced in response to the co-stimulation by IFNβ and TNFα in the absence of STAT1. Importantly, our results also confirm the contribution of distinct non-canonical STAT2 and/or IRF9-dependent pathway to the regulation of specific subsets of the IFNβ+TNFα-induced DEGs.

Differential regulation of *CXCL10* in response to IFNβ and IFNβ+TNFα.

Identification of DEGs upregulated by IFNβ+TNFα in a STAT1-independent, but STAT2 and IRF9-dependent, manner potentially reflects the regulation by an alternative STAT2/IRF9-containing complex (*4*, *7*). Whether this STAT2/IRF9 pathway ultimately leads to gene regulation through the same ISRE sites used by the ISGF3 complex remained to be assessed. In our RNASeq analysis (**Supplemental Table S1***)* and qRT-PCR validation (**Figure 4D**), *CXCL10* belongs to the IFNβ+TNFα-induced DEGs that are dependent on STAT2 and IRF9. The *CXCL10* promoter contains 3 ISRE sites. We used full-length wild-type (972bp containing the 3 ISRE sites), truncated (376bp containing only the ISRE(3) site) or mutated (972bp containing a mutated ISRE(3) site) *CXCL10* promoter luciferase (*CXCL10*prom-Luc) reporter constructs (**Figure 5**) to determine the ISRE consensus site(s) requirement. U3A cells were transfected with the *CXCL10*prom-Luc constructs and further stimulated with IFNβ+TNFα to study the STAT1-independent response. Additionally, STAT1 rescued U3A cells, U3AR, were transfected with the *CXCL10*prom-Luc constructs before stimulation with IFNβ to monitor the ISGF3-dependent response. As shown in **Figure 5**, induction of *CXCL10*prom in response to IFNβ in U3AR cells involves the distal ISRE(1) and/or ISRE(2) sites and the proximal ISRE(3) site. In contrary, only the ISRE(3) site is required for induction by

IFNβ+TNFα in U3A cells. Interestingly we also assessed the contribution of the two NF-κB and the AP-1 sites present in the promoter using *CXCL10*prom-Luc mutated constructs in comparison to the wild-type reporter. While none of the NF-κB and the AP-1 sites were required for induction of the *CXCL10* promoter by IFNβ in U3AR cells, the two NF-κB sites were necessary for the STAT1-independent induction in response to IFNβ+TNFα in U3A cells. These observations suggest that the ISRE site usage is more restricted in the absence of STAT1 in the context of the co-stimulation with IFNβ TNFα than in the context of an ISGF3-dependent regulation.

DISCUSSION

Our study was designed to determine the functional relevance of a STAT1-independent, but STAT2- and IRF9-dependent, signaling pathway in the transcriptional program induced by IFNβ in the presence of TNFα. Previous studies reported that IFNβ and TNFα synergize to induce a specific delayed antiviral program that differs from the response induced by IFNβ only. This specific synergy-dependent antiviral response is required for a complete abrogation of Myxoma virus in fibroblasts (*10*) and contributes to the establishment of a sustained type I and type III IFNs response during paramyxovirus infection in airway epithelial cells (*12*). The underlying mechanisms of this specific response remain ill defined, but their elucidation is of particular importance with regards to conditions with elevated levels of both IFNβ and TNFα such as pathogen intrusion or, autoimmune or chronic inflammatory diseases (*8*).

First, we confirmed the previously documented synergistic induction of an IFNβ+TNFα-mediated delayed transcriptional program composed of genes that are either not responsive to IFNβ or TNFα separately or are only responsive to either one of the cytokine when used separately albeit to a lesser extent (**Figure 1**). Using genome wide RNA sequencing, we demonstrate that IFNβ+TNFα induces a broad transcriptional program in cells deficient in STAT1. GO enrichment and transcriptional module analyses showed that STAT1-independent upregulated DEGs encompass a wide range of immunoregulatory and host defense, mainly antiviral, functions. These findings highlight the functional significance of a STAT1-independent response.

In the present study, we focused on deciphering the role of STAT2 and IRF9 in the STAT1-independent transcriptional program elicited in response to IFNβ+TNFα. We previously found that IFNβ+TNFα induce *DUOX2* via a STAT2/IRF9 pathway in the absence of STAT1 (*12*). To what extent this pathway contributes to the STAT1-independent response engaged downstream of IFNβ+TNFα remained to be addressed. Based on the possible regulation by STAT2 and/or IRF9, IFNβ+TNFα-induced DEGs could theoretically partitioned into 9 different predicted categories (**Figure 2E**), but we found that they in fact only significantly segregate into 7 categories. Importantly, the distribution of DEGs amongst 7 different categories reflects distinct contributions of STAT2 or IRF9 and highlights the heterogeneity of the mechanisms of regulation of the IFNβ+TNFα-induced genes. Importantly, only one anecdotic gene was found in categories implying inverse regulation by STAT2 and IRF9 (categories H and I) pointing to convergent functions of STAT2 and IRF9 when both are engaged in gene regulation. We can rule out that the distinct regulation mechanisms reflect distinct profiles of induction by IFNβ+TNFα. For instance *CXCL10*, *IL33*, *CCL20* and *ISG20* all exhibit synergistic induction by IFNβ+TNFα (**Figure 1**), but are differentially regulated by STAT2 and/or IRF9; while *CXCL10* is dependent on STAT2 and IRF9, *IL33* is independent on STAT2 and IRF9, and *CCL20* and *ISG20* are STAT2-independent but IRF9-dependent (**Figure 4D**).

Consistent with our previous report (*12*), we found several genes positively regulated by a non-canonical STAT2- and IRF9-dependent, but STAT1-independent, pathway (Category A). DEGs in this category encompass most of the functions induced in response to IFNβ+TNFα, with the notable exception of cell cycle and growth arrest and inflammasome and receptor signaling functions. Genes negatively regulated by STAT2 and IRF9 were also identified (Category B). Accumulating evidence point to the formation of an alternative STAT2/IRF9-containing complex mediating gene expression in the absence of STAT1 (*31-35*). The specificity of the DNA-binding of a STAT2/IRF9 complex compared to the ISGF3 complex remains unclear. It was originally found that STAT2/IRF9 exhibit only limited DNA-binding affinity for the typical ISRE sequence in the absence of STAT1 (*31*), but association of STAT2 with the promoter of antiviral genes induced by Dengue virus in STAT1-deficient mice was demonstrated by Chromatin immunoprecipitation (*36*). Here, the *CXCL10* gene was further analyzed as a paradigm of STAT2- and IRF9- positively regulated gene. Promoter activity analysis unveiled distinct ISRE site usage between IFNβ and IFNβ+TNFα stimulation (**Figure 5**). Interestingly, the ISRE site used in response to IFNβ+TNFα lies close to the NF-κB sites that are also specifically engaged in this response. A possible mechanism for the synergistic action of IFNβ+TNFα might be related to the previous description of the cooperativity between ISGF3 and NF-κB in the context of Listeria infection (*37, 38*). In this context, ISGF3 and NF-κB tether a complete functional mediator multi-subunit complex that bridges transcription factors with Pol II and initiation and elongation factors to the promoter of antimicrobial genes (*37*). Both STAT1 and STAT2 functionally and physically interact with the mediator (*39, 40*). However, this mechanism, if it contributes to the synergistic induction of some IFNβ+TNFα-induced genes, cannot explain it all. Indeed, not all IFNβ+TNFα-induced DEGs harbor NF-κB binding sites in their promoter. For instance, the *IFIT1* promoter contains only two identifiable cis-acting elements corresponding to ISRE binding sites (*41*). Unless, unknown binding sites are involved in the recruitment of a yet to be identified transcription factor, we cannot exclude that specific regulation of STAT2 and IRF9 might contribute to the synergistic response elicited by IFNβ+TNFα. In a previous study, we observed IRF9 induction and enhanced/extended STAT2 phosphorylation in response to IFNβ+TNFα (*12*). We hypothesized that these events likely contribute to the specific activation of the non-canonical STAT2/IRF9-dependent pathway. Remarkably, a similar prolonged STAT2 phosphorylation was observed upon stimulation of STAT1 KO bone marrow–derived murine macrophages with IFNα. In this context, a STAT2/IRF9 complex was shown to induce a delayed set of ISGs (*35*). Taken together, it is reasonable to speculate that in a physiological context, when TNFα is present with IFNβ, a signal is elicited to progressively exclude STAT1 from the STAT2/IRF9 complex and favor the non-canonical STAT2/IRF9 pathway to drive a specific delayed response.

The observation that some IFNβ+TNFα-induced genes were independent of IRF9 but dependent on STAT2, either positively or negatively, in a STAT1 deficient context (Categories D and E) might reflect the previous observation that STAT2 forms alternative complexes with other STAT members. STAT2 was shown to associate with STAT3 and STAT6, although it is not completely clear whether IRF9 is also required in these alternative complexes (*42, 43*). Interestingly, transcriptional module analyses demonstrated that the functional distribution of genes negatively regulated by STAT2 is very limited compared to other categories; only a virus-sensing module was enriched in this category. In contrary, IRF9-independent genes positively regulated by STAT2 mediate broader antiviral and immunoregulatory functions.

ISGF3-independent functions of IRF9 have been proposed based on the study of IRF9 deficiencies (reviewed in (*7, 44*)). However, IRF9 target genes in these contexts have been barely

documented. Intriguingly, Li et al. (*45*) studied IFNα-induced genes and their dependency on the ISGF3 subunits. While they confirmed previous studies showing IFNα can trigger a delayed and sustained ISGs response via an ISGF3-independent pathway, it is very striking that they did not find STAT1- and STAT2-independent but IRF9-dependent genes. Indeed, all identified IRF9-dependent genes were either STAT2- or STAT1-dependent. This result greatly differs with our study. Here, we found several IFNβ+TNFα-induced DEGs independent of STAT1 and STAT2, but positively or negatively regulated by IRF9 (Categories F and G). Typically IRF9 is considered a positive regulator of gene transcription. However, our findings are consistent with recent reports documenting the role of IRF9 in the negative regulation of the TRIF/NF-κB transcriptional response (*46*) or the expression of SIRT1 in acute myeloid leukemia cells (*47*). The molecular mechanism underlying gene regulation by IRF9 without association with either STAT1 or STAT2 remain to be elucidated. To the best of our knowledge, no alternative IRF9-containing complex has been described.

Unexpectedly, a vast majority of genes were found to be independent of STAT2 and IRF9 (Categorie C). All transcriptional modules were enriched in this category pointing to a major role of a yet to be identified pathway in the establishment of a host defense and immunoregulatory response. The NF-κB pathway is widely known to be engaged downstream of the TNF receptor While NF-κB is an obvious candidate for being involved in the regulation of the STAT2 and IRF9-independent DEGs, this might fall short in explaining the synergistic action of IFNβ+TNFα. Synergistic activation of NF-κB was reported in the context of IFNγ and TNFα treatment (*48*). However, we did not observe enhanced NF-κB activation upon IFNβ+TNFα stimulation compared to TNFα alone (*12*). Alternative pathways might be of interest. For instance, the *IL33* gene is synergistically induced by IFNβ+TNFα in a STAT2 and IRF9-independent manner; scanning of the *IL33* promoter for transcription factor binding sites revealed AP-1, NF-κB and IRF7 consensus sites (*49*). The potential role of AP-1 is also supported by the finding that the AP-1 transcription network module is enriched amongst IFNβ+TNFα-induced DEGs (**Figure 4E**). However, this module is not restricted to genes regulated independently of STAT2 and IRF9. It is also worth noting that two modules of IRF2-target genes were enriched, although again not specifically in the STAT2- and IRF-9 independent category (**Figure 4E**). Further studies will challenge the role of these transcription factors in the synergistic induction of genes by IFNβ+TNFα independently of STAT2 and IRF9.

Altogether our results demonstrate that in conditions with elevated levels of IFNβ and TNFα, a broad antiviral and immunoregulatory delayed transcriptional program is elicited independently of STAT1. While a substantial portion of this response is mediated by yet to be deciphered STAT2- and IRF9-independent mechanisms, our findings highlight the importance of diverse non-canonical STAT2 and/or IRF9 pathways. Consistent with the growing literature, IFNβ and TNFα synergistic action is in part mediated by the concerted action of STAT2 and IRF9, most likely present in an alternative complex. Finally, our study reveals specific independent roles of STAT2 and IRF9 in the regulation of distinct sets of IFNβ and TNFα-induced genes.

Conflict of Interest

The authors declare that the research was conducted in the absence of any commercial or financial relationships that could be construed as a potential conflict of interest.

Author Contributions

MM and NG conceived and designed the experiments. MM, AF, MK, EC, AH, EM and SC performed experiments. PD and AS performed bioinformatics analysis. MM and NG analyzed the data. NG wrote the manuscript. All co-authors edited and approved the manuscript.

Funding

The present work was funded by grants from Natural Sciences and Engineering Research Council of Canada (NSERC, #355306) and by the Research Chair in signaling in virus infection and oncogenesis from the Université de Montréal to NG. AS acknowledges funds from the University of Montreal, NSERC and the Merck Foundation. SCO was the recipient of a MITACS Globalink studentship. NG was recipient of a Tier II Canada Research Chair.

Acknowledgements

We are very thankful to Dr. D. Proud, University of Calgary and Dr. G. Stark, Cleveland clinic, for sharing reagents used in this study. RNASeq analyses were performed at the McGill University and Génome Québec Innovation Centre.

References

1. F. McNab, K. Mayer-Barber, A. Sher, A. Wack, A. O'Garra, Type I interferons in infectious disease. *Nat Rev Immunol* **15**, 87-103 (2015).
2. E. Tomasello, E. Pollet, T. P. Vu Manh, G. Uze, M. Dalod, Harnessing Mechanistic Knowledge on Beneficial Versus Deleterious IFN-I Effects to Design Innovative Immunotherapies Targeting Cytokine Activity to Specific Cell Types. *Frontiers in immunology* **5**, 526 (2014).
3. D. E. Levy, I. J. Marie, J. E. Durbin, Induction and function of type I and III interferon in response to viral infection. *Curr Opin Virol* **1**, 476-486 (2011).
4. K. Fink, N. Grandvaux, STAT2 and IRF9: Beyond ISGF3. *JAKSTAT* **2**, e27521 (2013).
5. W. M. Schneider, M. D. Chevillotte, C. M. Rice, Interferon-stimulated genes: a complex web of host defenses. *Annual review of immunology* **32**, 513-545 (2014).
6. N. Au-Yeung, R. Mandhana, C. M. Horvath, Transcriptional regulation by STAT1 and STAT2 in the interferon JAK-STAT pathway. *JAKSTAT* **2**, e23931 (2013).
7. A. Majoros, E. Platanitis, E. Kernbauer-Holzl, F. Rosebrock, M. Muller, T. Decker, Canonical and Non-Canonical Aspects of JAK-STAT Signaling: Lessons from Interferons for Cytokine Responses. *Frontiers in immunology* **8**, 29 (2017).
8. T. Cantaert, D. Baeten, P. P. Tak, L. G. van Baarsen, Type I IFN and TNFalpha cross-regulation in immune-mediated inflammatory disease: basic concepts and clinical relevance. *Arthritis Res Ther* **12**, 219 (2010).
9. J. Mestan, M. Brockhaus, H. Kirchner, H. Jacobsen, Antiviral activity of tumour necrosis factor. Synergism with interferons and induction of oligo-2',5'-adenylate synthetase. *J Gen Virol* **69 (Pt 12)**, 3113-3120 (1988).
10. E. Bartee, M. R. Mohamed, M. C. Lopez, H. V. Baker, G. McFadden, The addition of tumor necrosis factor plus beta interferon induces a novel synergistic antiviral state against poxviruses in primary human fibroblasts. *J Virol* **83**, 498-511 (2009).
11. A. Yarilina, K. H. Park-Min, T. Antoniv, X. Hu, L. B. Ivashkiv, TNF activates an IRF1-dependent autocrine loop leading to sustained expression of chemokines and STAT1-dependent type I interferon-response genes. *Nat Immunol* **9**, 378-387 (2008).

12. K. Fink, L. Martin, E. Mukawera, S. Chartier, X. De Deken, E. Brochiero, F. Miot, N. Grandvaux, IFNbeta/TNFalpha synergism induces a non-canonical STAT2/IRF9-dependent pathway triggering a novel DUOX2 NADPH oxidase-mediated airway antiviral response. *Cell Res* **23**, 673-690 (2013).
13. R. McKendry, J. John, D. Flavell, M. Muller, I. M. Kerr, G. R. Stark, High-frequency mutagenesis of human cells and characterization of a mutant unresponsive to both alpha and gamma interferons. *Proc Natl Acad Sci U S A* **88**, 11455-11459 (1991).
14. A. C. Robitaille, M. K. Mariani, A. Fortin, N. Grandvaux, A High Resolution Method to Monitor Phosphorylation-dependent Activation of IRF3. *J Vis Exp*, e53723 (2016).
15. A. A. Dussault, M. Pouliot, Rapid and simple comparison of messenger RNA levels using real-time PCR. *Biol Proced Online* **8**, 1-10 (2006).
16. A. M. Bolger, M. Lohse, B. Usadel, Trimmomatic: a flexible trimmer for Illumina sequence data. *Bioinformatics* **30**, 2114-2120 (2014).
17. A. Dobin, C. A. Davis, F. Schlesinger, J. Drenkow, C. Zaleski, S. Jha, P. Batut, M. Chaisson, T. R. Gingeras, STAR: ultrafast universal RNA-seq aligner. *Bioinformatics* **29**, 15-21 (2013).
18. A. Roberts, H. Pimentel, C. Trapnell, L. Pachter, Identification of novel transcripts in annotated genomes using RNA-Seq. *Bioinformatics* **27**, 2325-2329 (2011).
19. C. Trapnell, D. G. Hendrickson, M. Sauvageau, L. Goff, J. L. Rinn, L. Pachter, Differential analysis of gene regulation at transcript resolution with RNA-seq. *Nat Biotechnol* **31**, 46-53 (2013).
20. S. Anders, W. Huber, Differential expression analysis for sequence count data. *Genome Biol* **11**, R106 (2010).
21. M. D. Robinson, D. J. McCarthy, G. K. Smyth, edgeR: a Bioconductor package for differential expression analysis of digital gene expression data. *Bioinformatics* **26**, 139-140 (2010).
22. M. D. Young, M. J. Wakefield, G. K. Smyth, A. Oshlack, Gene ontology analysis for RNA-seq: accounting for selection bias. *Genome Biol* **11**, R14 (2010).
23. J. Weiner, T. Domaszewska, tmod: an R package for general and multivariate enrichment analysis. *PeerJ Preprints*, 4:e2420v2421 (2016).
24. Z. Bar-Joseph, G. K. Gerber, T. I. Lee, N. J. Rinaldi, J. Y. Yoo, F. Robert, D. B. Gordon, E. Fraenkel, T. S. Jaakkola, R. A. Young, D. K. Gifford, Computational discovery of gene modules and regulatory networks. *Nat Biotechnol* **21**, 1337-1342 (2003).
25. D. Chaussabel, N. Baldwin, Democratizing systems immunology with modular transcriptional repertoire analyses. *Nat Rev Immunol* **14**, 271-280 (2014).
26. D. Chaussabel, C. Quinn, J. Shen, P. Patel, C. Glaser, N. Baldwin, D. Stichweh, D. Blankenship, L. Li, I. Munagala, L. Bennett, F. Allantaz, A. Mejias, M. Ardura, E. Kaizer, L. Monnet, W. Allman, H. Randall, D. Johnson, A. Lanier, M. Punaro, K. M. Wittkowski, P. White, J. Fay, G. Klintmalm, O. Ramilo, A. K. Palucka, J. Banchereau, V. Pascual, A modular analysis framework for blood genomics studies: application to systemic lupus erythematosus. *Immunity* **29**, 150-164 (2008).
27. S. Li, N. Rouphael, S. Duraisingham, S. Romero-Steiner, S. Presnell, C. Davis, D. S. Schmidt, S. E. Johnson, A. Milton, G. Rajam, S. Kasturi, G. M. Carlone, C. Quinn, D. Chaussabel, A. K. Palucka, M. J. Mulligan, R. Ahmed, D. S. Stephens, H. I. Nakaya, B. Pulendran, Molecular signatures of antibody responses derived from a systems biology study of five human vaccines. *Nat Immunol* **15**, 195-204 (2014).
28. Y. Benjamini, Y. Hochberg, Controlling the False Discovery Rate: A Practical and Powerful Approach to Multiple Testing *Journal of the Royal Statistical Society. Series B (Methodological)* **57**, 289-300 (1995).

29. I. Ross, R. Gentleman, R: a language for data analysis and graphics. *Journal of computational and graphical statistics.* **5.3**, 299-314 (1996).
30. R. S. Zaheer, R. Koetzler, N. S. Holden, S. Wiehler, D. Proud, Selective transcriptional down-regulation of human rhinovirus-induced production of CXCL10 from airway epithelial cells via the MEK1 pathway. *J Immunol* **182**, 4854-4864 (2009).
31. H. A. Bluyssen, D. E. Levy, Stat2 is a transcriptional activator that requires sequence-specific contacts provided by stat1 and p48 for stable interaction with DNA. *J Biol Chem* **272**, 4600-4605 (1997).
32. M. Martinez-Moczygemba, M. J. Gutch, D. L. French, N. C. Reich, Distinct STAT structure promotes interaction of STAT2 with the p48 subunit of the interferon-alpha-stimulated transcription factor ISGF3. *J Biol Chem* **272**, 20070-20076 (1997).
33. S. Gupta, M. Jiang, A. B. Pernis, IFN-alpha activates Stat6 and leads to the formation of Stat2:Stat6 complexes in B cells. *J Immunol* **163**, 3834-3841 (1999).
34. Y. J. Lou, X. R. Pan, P. M. Jia, D. Li, S. Xiao, Z. L. Zhang, S. J. Chen, Z. Chen, J. H. Tong, IRF-9/STAT2 [corrected] functional interaction drives retinoic acid-induced gene G expression independently of STAT1. *Cancer Res* **69**, 3673-3680 (2009).
35. A. A. Abdul-Sater, A. Majoros, C. R. Plumlee, S. Perry, A. D. Gu, C. Lee, S. Shresta, T. Decker, C. Schindler, Different STAT Transcription Complexes Drive Early and Delayed Responses to Type I IFNs. *J Immunol* **195**, 210-216 (2015).
36. S. T. Perry, M. D. Buck, S. M. Lada, C. Schindler, S. Shresta, STAT2 mediates innate immunity to Dengue virus in the absence of STAT1 via the type I interferon receptor. *PLoS Pathog* **7**, e1001297 (2011).
37. S. Wienerroither, P. Shukla, M. Farlik, A. Majoros, B. Stych, C. Vogl, H. Cheon, G. R. Stark, B. Strobl, M. Muller, T. Decker, Cooperative Transcriptional Activation of Antimicrobial Genes by STAT and NF-kappaB Pathways by Concerted Recruitment of the Mediator Complex. *Cell Rep* **12**, 300-312 (2015).
38. M. Farlik, B. Reutterer, C. Schindler, F. Greten, C. Vogl, M. Muller, T. Decker, Nonconventional initiation complex assembly by STAT and NF-kappaB transcription factors regulates nitric oxide synthase expression. *Immunity* **33**, 25-34 (2010).
39. J. F. Lau, I. Nusinzon, D. Burakov, L. P. Freedman, C. M. Horvath, Role of metazoan mediator proteins in interferon-responsive transcription. *Mol Cell Biol* **23**, 620-628 (2003).
40. N. Zakharova, E. S. Lymar, E. Yang, S. Malik, J. J. Zhang, R. G. Roeder, J. E. Darnell, Jr., Distinct transcriptional activation functions of STAT1alpha and STAT1beta on DNA and chromatin templates. *J Biol Chem* **278**, 43067-43073 (2003).
41. V. Fensterl, G. C. Sen, The ISG56/IFIT1 gene family. *J Interferon Cytokine Res* **31**, 71-78 (2011).
42. L. Wan, C. W. Lin, Y. J. Lin, J. J. Sheu, B. H. Chen, C. C. Liao, Y. Tsai, W. Y. Lin, C. H. Lai, F. J. Tsai, Type I IFN induced IL1-Ra expression in hepatocytes is mediated by activating STAT6 through the formation of STAT2: STAT6 heterodimer. *J Cell Mol Med* **12**, 876-888 (2008).
43. J. J. Ghislain, E. N. Fish, Application of genomic DNA affinity chromatography identifies multiple interferon-alpha-regulated Stat2 complexes. *J Biol Chem* **271**, 12408-12413 (1996).
44. T. Suprunenko, M. J. Hofer, The emerging role of interferon regulatory factor 9 in the antiviral host response and beyond. *Cytokine Growth Factor Rev* **29**, 35-43 (2016).
45. W. Li, M. J. Hofer, P. Songkhunawej, S. R. Jung, D. Hancock, G. Denyer, I. L. Campbell, Type I interferon-regulated gene expression and signaling in murine mixed glial cells lacking signal transducers and activators of transcription 1 or 2 or interferon regulatory factor 9. *J Biol Chem* **292**, 5845-5859 (2017).

46. X. Zhao, Q. Chu, J. Cui, R. Huo, T. Xu, IRF9 as a negative regulator involved in TRIF-mediated NF-kappaB pathway in a teleost fish, Miichthys miiuy. *Mol Immunol* **85**, 123-129 (2017).
47. W. L. Tian, R. Guo, F. Wang, Z. X. Jiang, P. Tang, Y. M. Huang, L. Sun, IRF9 inhibits human acute myeloid leukemia through the SIRT1-p53 signaling pathway. *FEBS Lett*, (2017).
48. J. L. Cheshire, A. S. Baldwin, Jr., Synergistic activation of NF-kappaB by tumor necrosis factor alpha and gamma interferon via enhanced I kappaB alpha degradation and de novo I kappaBbeta degradation. *Mol Cell Biol* **17**, 6746-6754 (1997).
49. L. Sun, Z. Zhu, N. Cheng, Q. Yan, R. D. Ye, Serum amyloid A induces interleukin-33 expression through an IRF7-dependent pathway. *Eur J Immunol* **44**, 2153-2164 (2014).

Figure legends

Figure. 1: Expression of a panel of antiviral and immunoregulatory genes in response to IFNβ, TNFα and IFNβ+TNFα.

A549 cells were stimulated with either TNFα (10ng/mL), IFNβ (1000U/mL) or costimulated with IFNβ+TNFα (1000U/mL and 10ng/mL, respectively) for the indicated times. Quantification of mRNA was performed by qRT-PCR and expressed as relative expression (ΔΔCt) after normalization to the S9 mRNA levels. Mean +/- SEM, n≥3. Statistical comparison of TNFα *vs.* IFNβ+TNFα and IFNβ *vs.* IFNβ+TNFα was conducted using two-way ANOVA with Tukey's post-test. $P < 0.01$ (**), $P < 0.001$ (***) or $P < 0.0001$ (****).

Figure 2: Experimental design used to study the STAT1-independent delayed transcriptional program induced by the combination of IFNβ and TNFα.

A) U3A cells (STAT1-deficient) and U3AR cells (reconstituted U3A cells expressing STAT1) were left untreated or stimulated with IFNβ+TNFα (1000U/ml and 10ng/ml, respectively) for the indicated times. WCE were analyzed by SDS-PAGE followed by immunoblot (IB) using anti STAT1-P-Tyr701, total STAT1, STAT2-P-Tyr690, total STAT2, IRF9 or actin antibodies. **B-E)** U3A cells were transfected with siCTRL, siSTAT2 or siIRF9 before being left untreated (NS) or stimulated with IFNβ+TNFα (1000U/ml and 10ng/ml, respectively) for 24h. **In B**, The schematic describes the workflow of sample preparation and analysis. **In C**, WCE were analyzed by SDS-PAGE followed by IB using anti STAT2, IRF9 and actin antibodies. **In D**, Graph showing the correlation between fold-changes (FC), measured by RNASeq and qRT-PCR for 13 genes. Data from siCTRL NS vs siCTRL IFNβ+TNFα, siSTAT2 IFNβ+TNFα vs siCTRL IFNβ+TNFα, siIRF9 IFNβ+TNFα vs siCTRL IFNβ+TNFα conditions were used. **In E**, Diagram describing the bioinformatics analysis strategy used to determine STAT1-independent differentially expressed genes (DEGs) and their regulation by STAT2 and IRF9.

Figure 3: Analysis of DEGs in STAT1-deficient U3A cells costimulated with IFNβ and TNFα.

A) Volcano plots of the fold-change (FC) *vs.* adjusted *P*-value of IFNβ+TNFα vs non-stimulated (NS) siCtrl conditions. **B)** Gene ontology (GO) enrichment analysis of the differentially upregulated genes in IFNβ+TNFα vs non-stimulated (NS) siCtrl conditions based on the Biological Processes and Molecular Function categories. **C)** Modular transcription analysis of upregulated DEGs. Eighteen enriched modules are shown. The full list of enriched modules is available **Supplemental Table S3.**

Figure 4: Clustering of IFNβ+TNFα-induced DEGs according to their regulation by STAT2 and IRF9.

A) Volcano plots of the fold-change *vs.* adjusted *P*-value of siSTAT2 IFNβ+TNFα *vs.* siCTRL IFNβ+TNFα conditions. **B)** Volcano plots of the fold-change *vs.* adjusted *P*-value of siIRF9 IFNβ+TNFα *vs.* siCTRL IFNβ+TNFα conditions. **C)** Hierarchical clustering of the categories of DEG responses according to their regulation by STAT2 and IRF9. Euclidean distance metric is used for the construction of distance matrix and the categories are used *a priori* input into clustering algorithm as detailed in Materials and Methods. **D)** Validation of DEGs regulation profile by qRT-PCR. U3A cells were transfected with siCTRL, siSTAT2 or siIRF9. Cells were further left untreated or stimulated with IFNβ+TNFα (1000U/ml and 10ng/ml, respectively) for 24h. Quantification of the mRNA corresponding to the indicated genes was performed by qRT-PCR and expressed as relative expression (ΔΔCt) after normalization to the S9 mRNA levels. Mean +/- SEM, n≥5. Statistical

comparison of siSTAT2 IFNβ+TNFα *vs* siCTRL IFNβ+TNFα and siIRF9 IFNβ+TNFα *vs* siCTRL IFNβ+TNFα conditions was conducted using one-way ANOVA with Dunett post-test. $P < 0.05$ (*), $P < 0.01$ (**), $P < 0.001$ (***) or $P < 0.0001$ (****). **E)** Diagram showing enriched transcription modules in each gene category.

Figure 5: Analysis of the *CXCL10* promoter regulation in response to IFNβ+TNFα vs IFNβ.
A) Schematic representation of the *CXCL10* promoter luciferase constructs used in this study indicating the main transcription factors consensus binding sites. **B)** U3A and U3AR cells were transfected with the indicated CXCL10prom-luciferase reporter constructs and either left untreated or stimulated with IFNβ (1000U/ml) or IFNβ+TNFα (1000U/ml and 10ng/ml, respectively). Relative luciferase activities were measured at 2416h post-stimulation and expressed as fold over the corresponding unstimulated condition. Mean +/- SEM, n=3. Data are representative of 3 independent experiments performed in triplicate. Statistical analyses were performed using an unpaired t-test comparing each promoter to the CXCL10prom-972bp contruct. $P < 0.01$ (**), $P < 0.001$ (***).

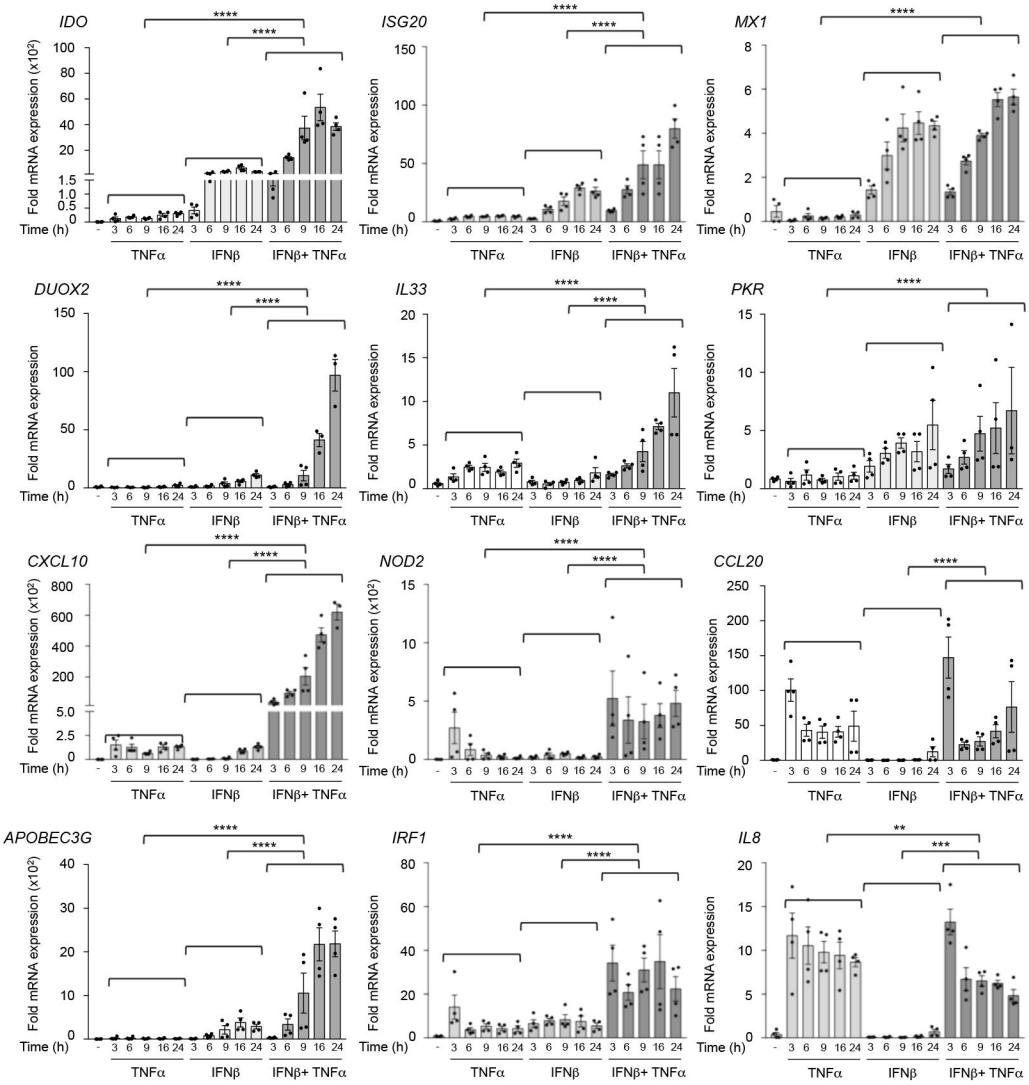
IDO
ISG20
MX1
DUOX2
IL33
PKR
CXCL10
NOD2
CCL20
APOBEC3G
IRF1
IL8
Fold mRNA expression (x10²)
Fold mRNA expression
Time (h)
- 3 6 9 16 24 3 6 9 16 24 3 6 9 16 24
TNFα
IFNβ
IFNβ+ TNFα
****
***
**

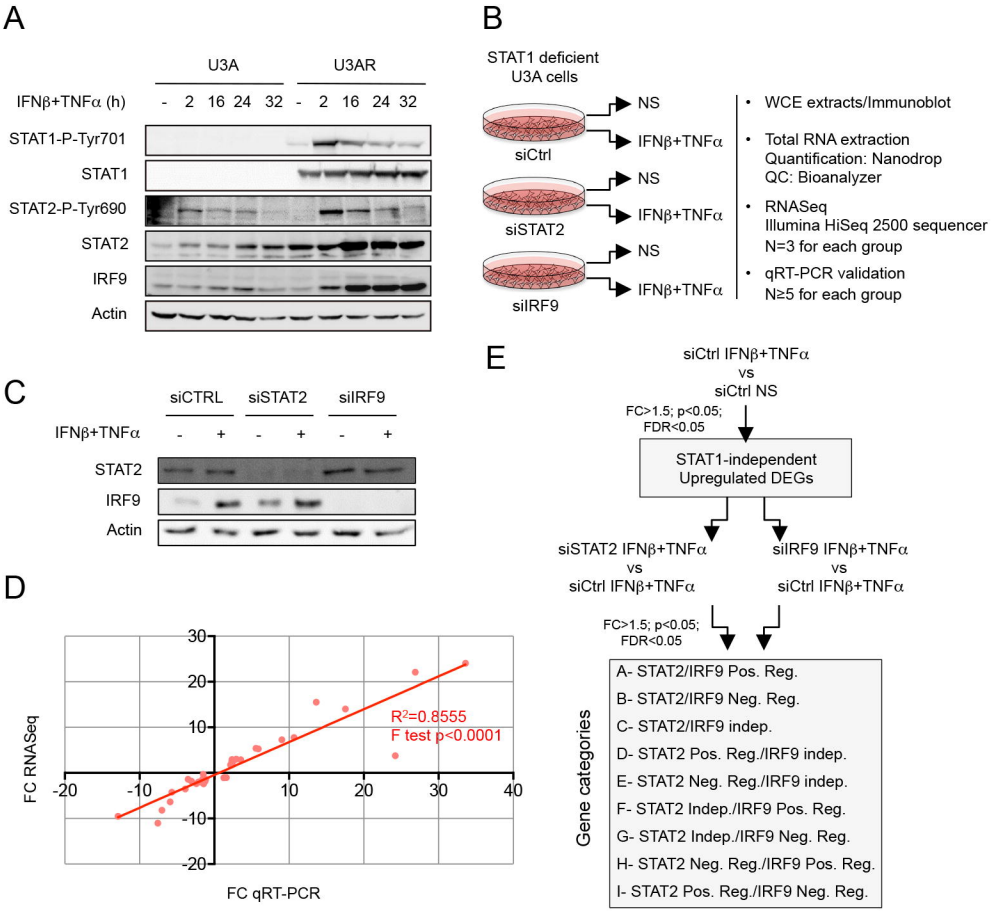
A
U3A
U3AR
IFNβ+TNFα (h)
- 2 16 24 32 - 2 16 24 32
STAT1-P-Tyr701
STAT1
STAT2-P-Tyr690
STAT2
IRF9
Actin
B
STAT1 deficient U3A cells
siCtrl
siSTAT2
siIRF9
NS
IFNβ+TNFα
• WCE extracts/Immunoblot
• Total RNA extraction
Quantification: Nanodrop
QC: Bioanalyzer
• RNASeq
Illumina HiSeq 2500 sequencer
N=3 for each group
• qRT-PCR validation
N≥5 for each group
C
siCTRL
siSTAT2
siIRF9
IFNβ+TNFα
- + - + - +
STAT2
IRF9
Actin
D
FC RNASeq
FC qRT-PCR
R²=0.8555
F test p<0.0001
E
siCtrl IFNβ+TNFα
vs
siCtrl NS
FC>1.5; p<0.05;
FDR<0.05
STAT1-independent
Upregulated DEGs
siSTAT2 IFNβ+TNFα
vs
siCtrl IFNβ+TNFα
siIRF9 IFNβ+TNFα
vs
siCtrl IFNβ+TNFα
FC>1.5; p<0.05;
FDR<0.05
Gene categories
A- STAT2/IRF9 Pos. Reg.
B- STAT2/IRF9 Neg. Reg.
C- STAT2/IRF9 indep.
D- STAT2 Pos. Reg./IRF9 indep.
E- STAT2 Neg. Reg./IRF9 indep.
F- STAT2 Indep./IRF9 Pos. Reg.
G- STAT2 Indep./IRF9 Neg. Reg.
H- STAT2 Neg. Reg./IRF9 Pos. Reg.
I- STAT2 Pos. Reg./IRF9 Neg. Reg.

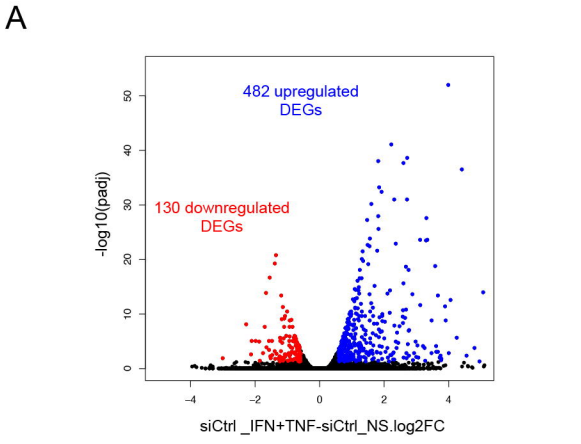
A
482 upregulated DEGs
130 downregulated DEGs
-log10(padj)
siCtrl _IFN+TNF-siCtrl_NS.log2FC

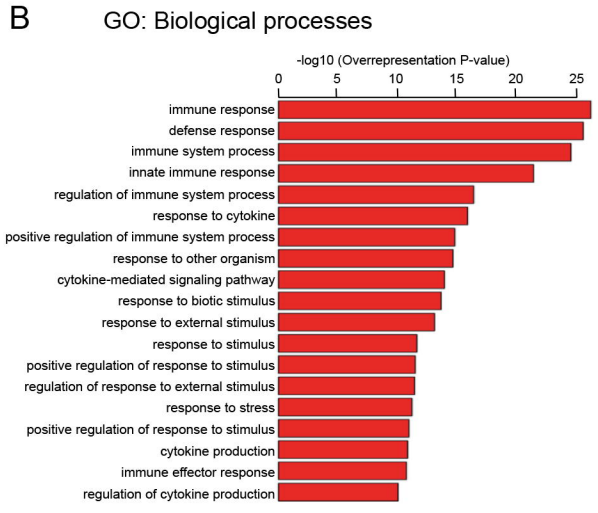
B
GO: Biological processes
-log10 (Overrepresentation P-value)
immune response
defense response
immune system process
innate immune response
regulation of immune system process
response to cytokine
positive regulation of immune system process
response to other organism
cytokine-mediated signaling pathway
response to biotic stimulus
response to external stimulus
response to stimulus
positive regulation of response to stimulus
regulation of response to external stimulus
response to stress
positive regulation of response to stimulus
cytokine production
immune effector response
regulation of cytokine production

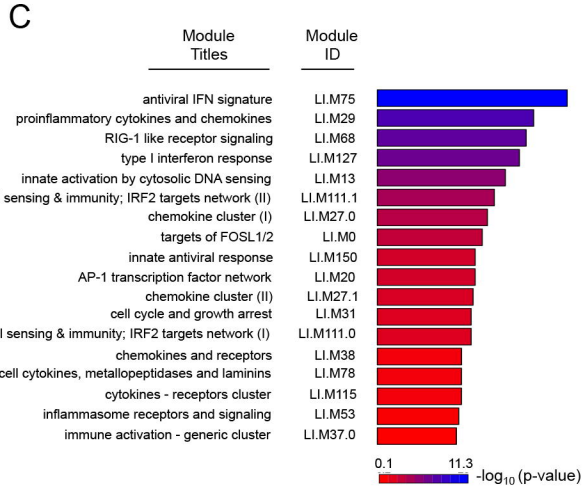
C
Module Titles
Module ID
antiviral IFN signature LI.M75
proinflammatory cytokines and chemokines LI.M29
RIG-1 like receptor signaling LI.M68
type I interferon response LI.M127
innate activation by cytosolic DNA sensing LI.M13
viral sensing & immunity; IRF2 targets network (II) LI.M111.1
chemokine cluster (I) LI.M27.0
targets of FOSL1/2 LI.M0
innate antiviral response LI.M150
AP-1 transcription factor network LI.M20
chemokine cluster (II) LI.M27.1
cell cycle and growth arrest LI.M31
viral sensing & immunity; IRF2 targets network (I) LI.M111.0
chemokines and receptors LI.M38
myeloid cell cytokines, metallopeptidases and laminins LI.M78
cytokines - receptors cluster LI.M115
inflammasome receptors and signaling LI.M53
immune activation - generic cluster LI.M37.0
0.1
11.3
-log10 (p-value)

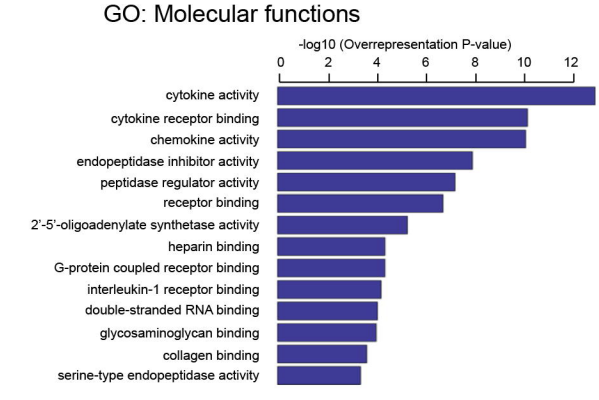
GO: Molecular functions
-log10 (Overrepresentation P-value)
cytokine activity
cytokine receptor binding
chemokine activity
endopeptidase inhibitor activity
peptidase regulator activity
receptor binding
2'-5'-oligoadenylate synthetase activity
heparin binding
G-protein coupled receptor binding
interleukin-1 receptor binding
double-stranded RNA binding
glycosaminoglycan binding
collagen binding
serine-type endopeptidase activity

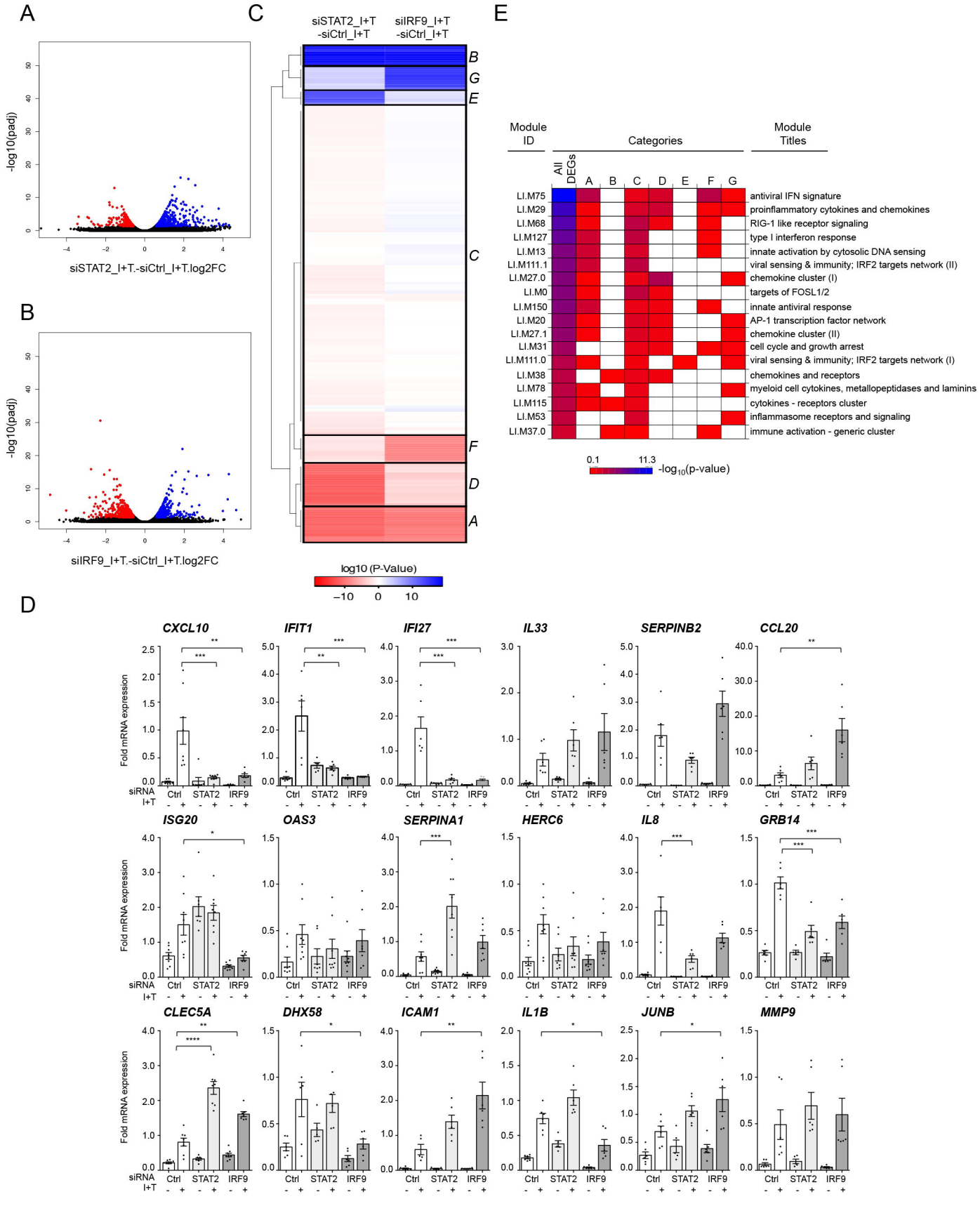
A
-log10(padj)
siSTAT2_I+T.-siCtrl_I+T.log2FC
B
-log10(padj)
siIRF9_I+T.-siCtrl_I+T.log2FC
C
siSTAT2_I+T -siCtrl_I+T
siIRF9_I+T -siCtrl_I+T
B
G
E
C
F
D
A
log10 (P-Value)
−10 0 10
E
Module ID
Categories
Module Titles
All DEGs
A B C D E F G
LI.M75 antiviral IFN signature
LI.M29 proinflammatory cytokines and chemokines
LI.M68 RIG-1 like receptor signaling
LI.M127 type I interferon response
LI.M13 innate activation by cytosolic DNA sensing
LI.M111.1 viral sensing & immunity; IRF2 targets network (II)
LI.M27.0 chemokine cluster (I)
LI.M0 targets of FOSL1/2
LI.M150 innate antiviral response
LI.M20 AP-1 transcription factor network
LI.M27.1 chemokine cluster (II)
LI.M31 cell cycle and growth arrest
LI.M111.0 viral sensing & immunity; IRF2 targets network (I)
LI.M38 chemokines and receptors
LI.M78 myeloid cell cytokines, metallopeptidases and laminins
LI.M115 cytokines - receptors cluster
LI.M53 inflammasome receptors and signaling
LI.M37.0 immune activation - generic cluster
0.1 11.3
-log10(p-value)
D
CXCL10
IFIT1
IFI27
IL33
SERPINB2
CCL20
ISG20
OAS3
SERPINA1
HERC6
IL8
GRB14
CLEC5A
DHX58
ICAM1
IL1B
JUNB
MMP9
Fold mRNA expression
siRNA Ctrl STAT2 IRF9
I+T

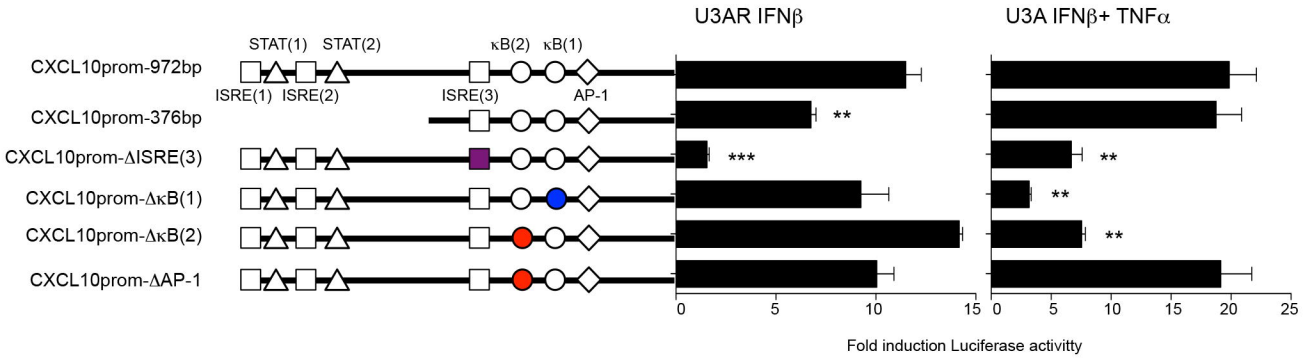
U3AR IFNβ
U3A IFNβ+ TNFα
STAT(1)
STAT(2)
κB(2)
κB(1)
ISRE(1)
ISRE(2)
ISRE(3)
AP-1
CXCL10prom-972bp
CXCL10prom-376bp
CXCL10prom-ΔISRE(3)
CXCL10prom-ΔκB(1)
CXCL10prom-ΔκB(2)
CXCL10prom-ΔAP-1
**
***
**
**
**
0
5
10
15
0
5
10
15
20
25
Fold induction Luciferase activitty